PCCP

View Online
Dynamic Article Links

Cite this: *Phys. Chem. Chem. Phys.*, 2011, **13**, 3721–3729

www.rsc.org/pccp

PAPER

Impact of concentration self-quenching on the charge generation yield of fullerene based donor–bridge–acceptor compounds in the solid state†

Mattias P. Eng,*[ab] Safa Shoaee,[a] Agustín Molina-Ontoria,[c] Andreas Gouloumis,[c] Nazario Martín*[cd] and James R. Durrant*[a]

Received 11th October 2010, Accepted 22nd November 2010
DOI: 10.1039/c0cp02107e

A fullerene based Donor–Bridge–Acceptor (DBA) compound, incorporating a π-extended tetrathiafulvalene electron donor, is investigated with respect to its photophysics in solution *versus* solid state. Solid films of neat DBA are compared with blend films where the DBA compound is diluted in the inert, low dielectric, polymer poly(styrene). It is found that the moderate intermolecular electronic coupling and donor–acceptor separation (22 Å) in this case leads to the generation of more dissociated, intermolecular charges than a mixture of the donor and acceptor reference compounds. However, the increased intermolecular interactions in the solid state lead to the excited state of the fullerene suffering from concentration self-quenching. This is found to severely affect the charge generation yield in solid films. The impact of competing intra and intermolecular interactions in the solid state upon the film photophysics is analysed in terms of a kinetic model which includes both the effects of concentration self-quenching and the impact of film composition upon the dielectric stabilisation of charge separated states. We conclude that both concentration self-quenching and dielectric stabilisation are critical in determining the photophysics of the blend films, and discuss strategies based upon our observations to enhance the charge photogeneration properties of organic films and photovoltaic devices based upon DBA compounds.

1. Introduction

Studies of the photophysics of molecular Donor–Bridge–Acceptor (DBA) systems in solution have made great progress in unravelling the fundamentals of electron transfer (ET) reactions in such systems. One of the long term goals of such research is to develop a general understanding of such processes for subsequent integration of these molecular systems in solid state devices, including photovoltaic (PV) solar cells, photoelectrodes for solar fuel generation and light emitting diodes. However, at present the correlation between the photophysics in solution and in solid state remains poorly determined. This is serving as a significant barrier between the fields of fundamental (solution) and applied (solid state) research and has motivated our interest in studying the effects on the photophysics of moving from solution to the solid state.[1,2] We here report a photophysical study of a fullerene based DBA system in solution and solid films to shed light on what photophysical parameters might be transferable from solution to the solid state.

Supramolecular systems based on the donor/acceptor approach have previously been used as the sole component in active layers for PV energy conversion with some success.[3–16] These studies have particularly been motivated by the potential ability of such systems to achieve structural control of the donor/acceptor interface on a molecular scale, something relatively difficult to achieve with more commonly used donor/acceptor blends. Achieving such molecular control of interface structure is likely to be the key to achieving efficient and predictable charge photogeneration.[17] Most supramolecular donor/acceptor systems utilize fullerene derivatives as final electron acceptors. The structures used as electron donors have either been short oligomers with the same repeat structure as that of polymers commonly used in bulk heterojunction based PV solar cells[3,4,6,11–13] or chromophores such as perylene diimide,[7] phthalocyanine,[5,8,15] π-extended tetrathiafulvalene (exTTF),[18] and azoaromatic[9,14,16] or cyanine[10] dyes. The highest

[a] *Department of Chemistry, Imperial College London, Exhibition Road, SW7 2AZ, London, UK. E-mail: j.durrant@imperial.ac.uk; Fax: +44 (0)2075945801; Tel: +44 (0)2075945321*
[b] *Department of Applied Physics, Chalmers University of Technology, Fysikgränd 3, 412 96, Göteborg, Sweden. E-mail: mattias.eng@chalmers.se; Fax: +46 317723134; Tel: +46 317725179*
[c] *Department of Organic Chemistry, Universidad Complutense de Madrid, Ciudad Universitaria, E-28040, Madrid, Spain. E-mail: nazmar@quim.ucm.es; Fax: +34 913944103; Tel: +34 913944227*
[d] *IMDEA-Nanociencia, E-28049 Madrid, Spain*

† Electronic supplementary information (ESI) available: Figures illustrating the quenching of triplets by oxygen, the turning off of charge generation in very dilute PS films, and the charge yield in films of **1** *vs.* a mixture of **2** and **3**. Also given is an in-depth description of the fitting procedure resulting in the lines in Fig. 10 and synthetic details. See DOI: 10.1039/c0cp02107e

total power conversion efficiency reported for solar cells using this type of photoactive layer is, to our knowledge, 0.37%.[9] Although not very impressive, it still gives promise for the approach as a potential new way for achieving cheap energy production. It also highlights the importance of in-depth studies of the photophysics of this type of compounds in the solid state since this will be imperative for systematically improving the efficiency.

We have previously reported to limited studies comparing the photophysics of DBA compounds in solution *versus* solid state.[1,2] In one study of structurally similar exTTF–fullerene based DBA compounds it was concluded that longer lived charge separated states in solution do not necessarily lead to a higher yield of long-lived free charge carriers in solid films.[2] Rather, it was found that the more conjugated compound, which exhibited a shorter lived charge separated state life-time in solution due to a higher electronic coupling, formed more free carriers in films. This was attributed to a higher propensity to form aggregates, enhancing intermolecular interactions which could drive intermolecular charge separation. Another factor might have been a longer donor–acceptor separation leading to a smaller coulomb barrier for charge dissociation. In another study perylene diimide and triphenylamine were used as the electron acceptor and donor, respectively.[1] For this system, it was concluded that the intramolecular electronic coupling between donor and acceptor was too large in relation to the intermolecular electronic coupling between donor/donor and acceptor/acceptor pairs in the solid film. This in effect led the charge separated state to act as an effective means of excited state deactivation rather than enhancing the generation of long lived free charges. On the contrary, a film of the acceptor reference compound gave a higher yield of free charges. In the present study we have therefore chosen a DBA compound with a moderate intramolecular electronic coupling (see Scheme 1). Here the donor is a π-extended tetrathiafulvalene (exTTF) and the acceptor is a methylpyrrolidinofullerene (C_{60}). The donor and acceptor are separated by a bridge containing a [2,2]paracyclophane moiety (pCP). This bridge unit has previously been shown to mediate efficiently intramolecular electron transfer whilst slowing down the charge recombination process.[19,20] In addition it has been shown to enable the formation of large ordered aggregates.[21] Previous studies of exTTF–Bridge–C_{60} DBA compounds in solution have shown that excitation of the fullerene can lead to the formation of the charge separated state.[22]

A key concern when comparing dilute solution *versus* solid state photophysics of molecular species is that intermolecular interactions in the solid state may result in enhanced non-radiative decay to ground—a process often referred to as 'concentration self-quenching' (discussed in detail below). Considering the exTTF–Bridge–C_{60} DBA addressed herein, it is known that the excited state decay dynamics of excited states of fullerene derivatives in solution is affected by the environment.[23] Additionally, studies of C_{60} have shown that the excitation of higher excited states—excitations to the lower states being formally forbidden—results, in the solid state, in a quenching of the fluorescence.[24,25] This has been suggested to be due to both a branching of the excited state decay dynamics to charge separated states and a scavenging effect of the introduction of charge transfer excitations. These hypotheses are corroborated by cyclic voltammetry of fullerene in solution that estimates the electrochemical HOMO–LUMO gap to be around 2.32 eV, less than the energy of these higher excited states.[26] Thus, there is the potential for the introduction of a $C_{60}^{\bullet -}$–$C_{60}^{\bullet +}$ charge separated state in the photophysics when the intermolecular interactions are substantial. From this it can be expected that the concentration self-quenching of fullerenes will have an impact on the solid state photophysics of fullerene based DBA compounds. Concentration self-quenching effect may also explain why the quantum efficiency of some fullerene/polymer bulk heterojunction solar cells shows an abrupt decrease in the UV.[27] A further consideration when comparing solution *versus* solid state photophysics of DBA systems is the impact on the energetics of charge separation due to the dielectric properties of the environment, which can result in large variations in the solvation or 'polarization' induced stabilisation of charge separated states relative to excited singlet and triplet states.[28,29]

In this paper, we investigate the interplay between concentration self-quenching and dielectric stabilisation upon the photophysics of the exTTF–Bridge–C_{60} DBA **1** (see Scheme 1) in solution and the solid state. We further studied the reference compounds **2** and **3** to allow comparison of solution *versus* solid state behaviour of the separated exTTF and C_{60} species.

2. Materials and methods

Solvents *o*-dichlorobenzene, benzonitrile, and toluene were purchased from Sigma-Aldrich and used as received. Solution

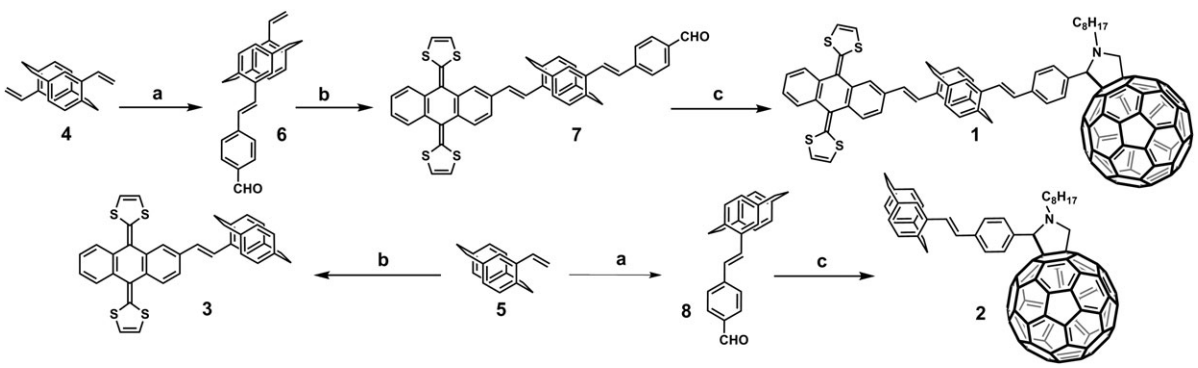

Scheme 1 Synthesis of dyad **1** and reference compounds **2** and **3**. *Reagents and conditions*: (a) 4-iodobenzaldehyde, $PdCl_2(MeCN)_2$, K_2CO_3, DMF, 100 °C, (b) iodo-exTTF, $PdCl_2(MeCN)_2$, K_2CO_3, DMF, 100 °C and (c) *N*-octylglycine, C_{60}, PhCl, reflux.

absorption and emission spectra were measured in 1 cm quartz cuvettes and transient absorption measurements were performed in a slightly bigger quartz cuvette with a septum to enable the use of deoxygenated environment. Oxygen was largely removed from the solution by leaving the cuvette open in a glove-box with nitrogen atmosphere for more than 30 min. In solution the concentration of the studied compound was kept below 4 μM to minimise intermolecular interactions. Thin films were spun cast on borosilicate glass substrates, cleaned by successive sonication for 15 min in acetone and then isopropanol, from 10 mg ml^{-1} *o*-dichlorobenzene solutions at a spin rate of 1500 rpm for 60 s. Absorption and photoluminescence (PL) spectra were measured with a spectrophotometer (Shimadzu, UV-1601) and a spectrofluorimeter (Horiba Jobin Yvon, Spex Fluoro-Log), respectively. Transient absorption data were collected on a setup employing pulsed excitation by either the fundamental from a nitrogen laser, 337 nm, or the tripled fundamental from a Nd:YAG laser, 355 nm, as detailed previously.[1,2] The relative dielectric constants at the low frequency limit, ε, of films of poly(styrene), poly(vinyl chloride) and **1** were measured by impedance spectroscopy (Solartron 1260 Gain/Phase Analyzer).

The synthesis of dyad **1** and reference compounds **2** and **3** was carried out by stepwise approaches based on the preparation of asymmetrically functionalized 4,12-divinyl-*pseudo*-paracyclophane endowed with a formyl group and an exTTF fragment at the terminal positions or from 4-vinylparacyclophane (Scheme 1, for details see ESI†). First, the preparation of intermediates **6** and **8**, carrying a terminal formyl group, was performed by using Pd-catalyzed cross-coupling reactions (Jeffery protocol)[30] between **4** or **5** and the commercially available 4-iodobenzaldehyde in yields of 47% and 70% respectively. The same Pd-catalyzed cross-coupling protocol was employed to obtain intermediate **7** and reference compound **3** starting from **6** or **5** respectively, and coupled to iodo-exTTF in moderate to good yields.

Finally, dyad **1** and reference **2** were obtained by 1,3-dipolar cycloaddition of the corresponding azomethine ylides, generated *in situ* from *N*-octylglycine and the corresponding aldehyde **7** or **8**, with C_{60}.[31,32] The products were obtained as brown solids in yields ranging from 42% and 66% respectively.

All quantum chemical calculations were performed using the Gaussian 03 software suite[33] using the 6-31G(d) basis set together with the B3LYP functional. Full optimizations were verified by frequency calculations that showed no virtual frequencies.

3. Results

Fig. 1 shows the normalised absorption spectrum of a dilute solution of **1** in toluene compared to the spectrum of a spin cast thin film. In the film there is evidence of aggregation, which appears as a relative increase in the C_{60} absorption in the red part of the spectrum. The effect of increased absorption in the red part of the spectrum has been observed previously, both for PCBM[24] and un-substituted fullerene.[25] This effect has been attributed to both the occurrence of charge transfer excitations and symmetry breaking. In addition to this, it is generally observed that the intensity of the UV absorption decreases

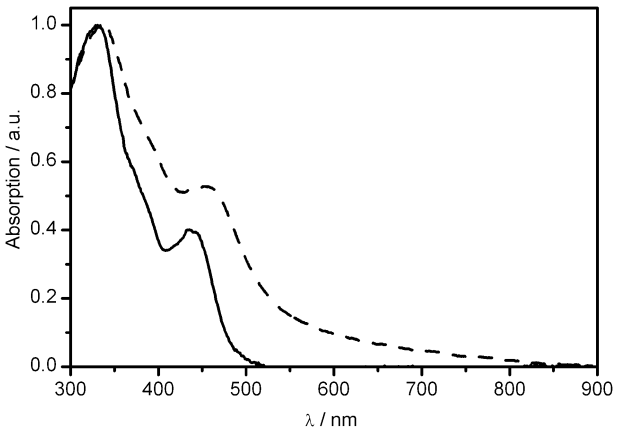

Fig. 1 Normalized absorption spectra of **1** in a dilute (4 μM) toluene solution (solid line) compared to a spin cast thin film (dashed line).

upon aggregation of fullerenes.[23] Upon closer examination the aggregation effects lead to a slight red shift of the exTTF absorption peak at around 440 nm. In addition, the peaks are broadened which is indicative of a more amorphous morphology. From solution spectroscopy of well ordered large aggregates a band narrowing effect is instead expected.[34] This is a good indication that the intermolecular interactions are random in nature, giving rise to a broad distribution of states in solid films.

We turn now to consideration of the excited state photophysics. We initially consider the solution photophysics, employing two different solvents: toluene and benzonitrile. Benzonitrile has a significantly higher dielectric constant than toluene ($\varepsilon \approx 25.8$ and 2.4 for benzonitrile and toluene, respectively), and is therefore expected to provide better solvation of photogenerated charge separated states. Exciting at 337 nm will mainly excite the C_{60} moiety and results in the characteristic fluorescence spectrum of fullerenes, with a maximum at around 715 nm. Fig. 2 illustrates that in toluene there is virtually no quenching of this emission whereas in benzonitrile there is a clear decrease of the C_{60} emission in **1** relative to the fullerene reference compound, **2**. This is a clear

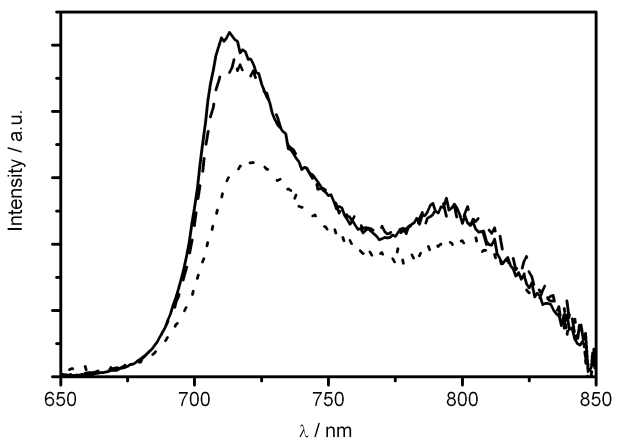

Fig. 2 Emission spectra in toluene from the reference compound **2** (solid line) and the DBA molecule **1** measured in toluene (dashed line) and benzonitrile (dotted line). All spectra are corrected for differences in sample absorption at the excitation wavelength (337 nm).

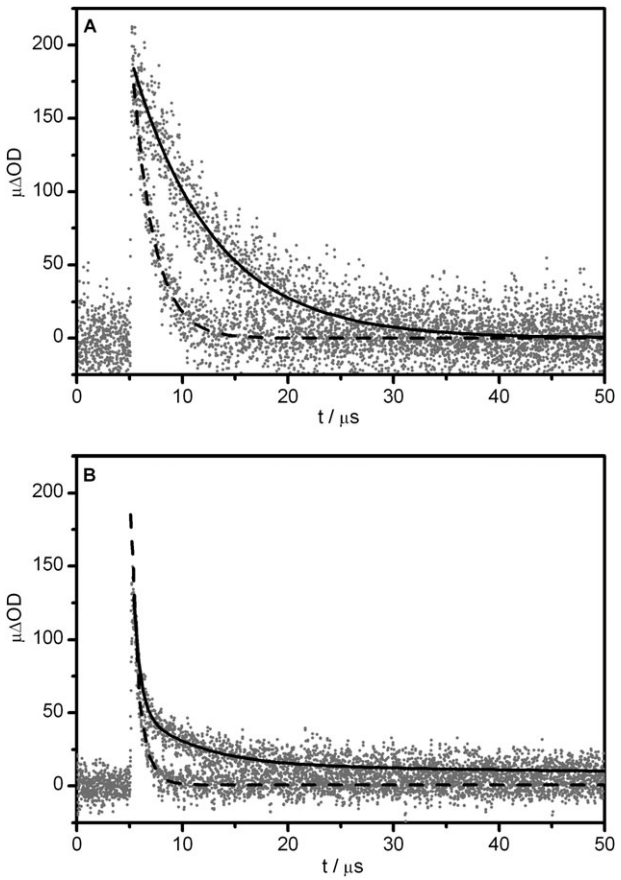

Fig. 3 The transient absorption decays at 690 nm of **1** in solutions that are either nitrogen purged (solid lines) or exposed to atmospheric oxygen (dashed lines) after 355 nm excitation in toluene (A) and benzonitrile (B).

indication that the origin of the fluorescence quenching in benzonitrile is due to electron transfer.

Fig. 3 shows transient absorption decays of **1** after exciting at 355 nm recorded in toluene and benzonitrile with and without oxygen. All decays were measured at a detection wavelength of 690 nm, corresponding to both exTTF$^{\bullet+}$ cation and C_{60} triplet absorption (see below). In toluene (Fig. 3A) only triplets were observed and the decay fits well to a mono-exponential decay with a life-time of around 7 μs that is significantly reduced in the presence of oxygen. In contrast, in the more polar benzonitrile three exponentials were required to fit the data (Fig. 3B). In line with the quenching of the fullerene fluorescence in this solvent, this suggests that a combination of radicals (life-time of about 500 ns) and triplets (life-time of about 7 μs and quenched in the presence of oxygen) is observed. Additionally there is a small contribution of a very long-lived component. The phenomenon of such a residual absorption has been observed previously for a structurally similar complex and was then assigned to two separate geometrical conformations of the DBA compound resulting in two different life times of the charge separated state.[35] However, in this case, the residual absorption is not observed in the presence of oxygen indicating that this feature is most likely due to, or originating from, a triplet species. Based on the absorption coefficients of the C_{60} triplet and the exTTF radical at this wavelength (see below) and the pre-exponential factors from the tri-exponential fit of the decay, the charge separation efficiency from the singlet excited state of C_{60} (hole transfer from C_{60} to exTTF) in benzonitrile solution is estimated to be approximately 40%. Thus in solution, compound **1** shows results that are consistent with previous studies on the impact of solvent polarity and bridge mediation on the kinetics of electron transfer in C60 based DBA compounds.[19,22,36–38]

Fig. 4 shows the transient absorption decays of **1** recorded in toluene and benzonitrile solutions compared to the decay recorded for a pristine solid film of **1**. From the figure it can be seen that in the solid state the formed charges are much more long lived than those in solution and follow a dispersive power law decay ($\Delta OD \propto t^{-\alpha}$, $\alpha \approx 0.3$) typical of trap-limited bimolecular recombination kinetics of diffusing charge carriers observed previously for organic semiconductor films.[39]

To get a deeper insight of the solid state photophysics, a series of thin films of **1** and **2** diluted in an inert PS matrix in various weight concentrations were studied. The absorption spectra showed a continuous increase in the red part of the spectrum as the concentration of the solute was increased, indicative of increased intermolecular interactions (not shown). Fig. 5 shows the red part of the mass-weighted emission spectra of films of **1** : PS with different weight fractions after exciting at 337 nm. As the figure clearly shows, the C_{60} emission is more and more quenched as the concentration in the solid film is increased.

The same quenching effect was also observed in films of the C_{60} control **2** diluted in PS with various weight fractions (not shown). Thus, it is most likely that there is a considerable contribution of concentration self-quenching to the overall decay of the C_{60} singlet state in both **1** and **2**. To investigate the impact of the concentration self-quenching on the charge generation yield transient absorption measurements were performed on solid films of **1** and **2** diluted in PS with various weight fractions.

Interestingly, the transient absorption decays of films of **1** diluted in PS show a combination of charges and triplets. The presence of triplets was verified by comparison of decays recorded in nitrogen and oxygen atmospheres (see Fig. S1 in the ESI†).

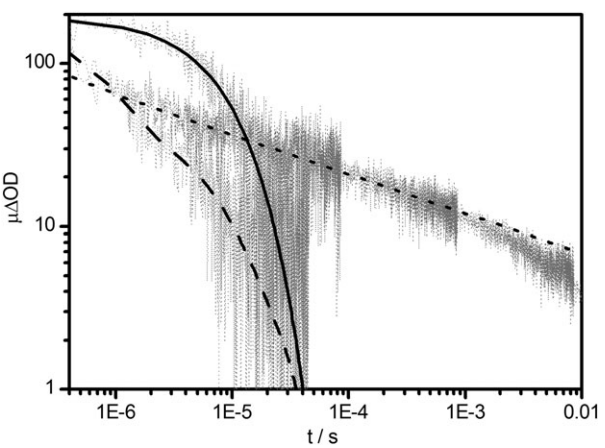

Fig. 4 Transient absorption decays of **1** (grey) together with fitted curves (lines) recorded in toluene (solid line), benzonitrile (dashed line), as a neat film (dotted line).

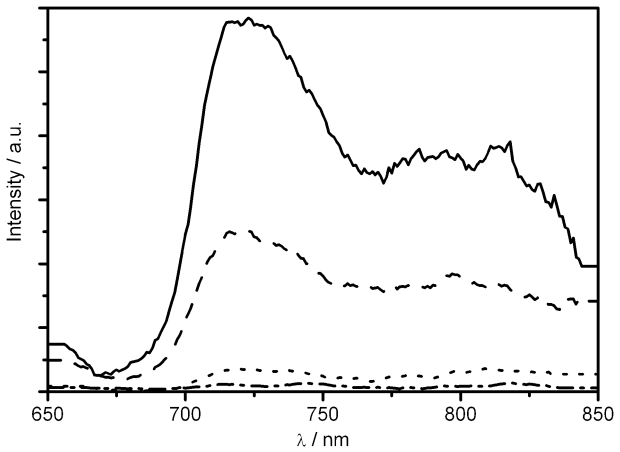

Fig. 5 Mass-weighted emission spectra of **1** : PS films with 10 : 90 (solid line), 20 : 80 (dashed line), 50 : 50 (dotted line), and 80 : 20 (dash-dotted line) w : w ratios.

The decay dynamics is then expected to be described by a combination of a power law describing the trap-limited bimolecular recombination of diffusing charges[39] and a single exponential describing triplet decay:

$$\Delta OD(t) = At^{-\alpha} + Be^{-t/\tau} \quad (1)$$

For the neat **1** film only the power law was required to fit the data, as illustrated in Fig. 4 above, and the presence of oxygen had no effect on the observed signal. Further information about the absorbing species in the films is revealed by examining the transient absorption spectra of the films (see Fig. 6). The transient absorption spectrum of the neat **1** film shows the well known features of the exTTF$^{\bullet+}$ cation radical with an absorption maximum at 680 nm ($\varepsilon \approx 25\,000$ M^{-1} cm^{-1})[22] and

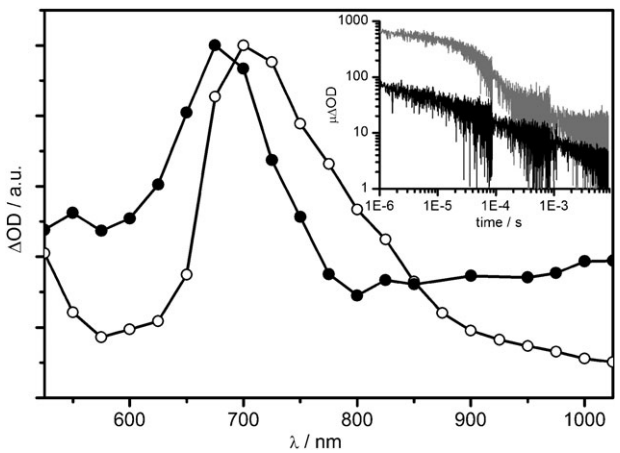

Fig. 6 The normalized transient absorption spectra of a neat **1** film (solid circles) and a 10 : 90 w : w **1** : PS film (open circles) after excitation with 337 nm. The spectra show the typical features of exTTF radical cations and C_{60} triplets, respectively. The inset shows the corresponding transients recorded at 690 nm for films containing neat **1** (black) and 10 : 90 w : w **1** : PS (grey). The neat film transient is dominated by the dispersive bimolecular recombination dynamics of dissociated charge carriers (first part of eqn (1)) whereas the low concentration transient is dominated by a monoexponential decay of fullerene triplets (second part of eqn (1)).

the $C_{60}^{\bullet-}$ anion radical with absorption at around 1000 nm ($\varepsilon \approx 10\,000$ M^{-1} cm^{-1}).[23] On the other hand, the spectrum of the dilute **1** : PS 10 : 90 w : w film shows the well known features of the $T_n \leftarrow T_0$ absorption spectrum for C_{60} with an absorption maximum at 710 nm ($\varepsilon \approx 16\,000$ M^{-1} cm^{-1}).[23] For all the films the two species are formed in parallel and there is no selective wavelength for probing either one. However, if decays are recorded at 690 nm, where both C_{60} triplets and exTTF radicals are probed, the proportions of each species can be extracted from combining fits of the decays to eqn (1) and the absorption coefficients of each species (see above).

In this way, to get a deeper insight into how the charge separation and concentration self-quenching processes compete, TAS decays were recorded for films containing various weight fractions of **1** and **2** in PS and the yields of charges and triplets determined. Comparing the yields of triplets and charges in films of **1** and **2** will allow for a quantitative estimation of the relative efficiencies of these processes as described in the ESI† and discussed in the next section of the paper. Fig. 7 shows fits of eqn (1) to TAS decays recorded for films of **1** in PS. From this figure it can be seen that increasing the concentration leads to less triplets forming (*i.e.* the fast phase), but also less charges (the power law decay is apparent as a straight line on this log : log plot at longer time delays). Thus it can be concluded that the efficiency of the self-quenching mechanism increases more with concentration than the efficiency of the charge separation. A more in-depth quantitative analysis will be made in the next section.

Fig. 8 shows the normalised signals for the triplet population determined from the fits of the transient absorption decays. Also shown is the integrated C_{60} emission intensities determined from the steady state emission data (Fig. 5). It is apparent that there is a very close correlation in the decrease in both triplet and singlet state yields. This is a clear indication that it is only the first excited singlet state that is affected by concentration self-quenching and that the inter-system crossing rate is unchanged. It also shows that the majority of triplets are generated *via* direct inter-system crossing from the singlet state and not *via* recombination of geminate or free charges, as has been observed in some cases.[40,41]

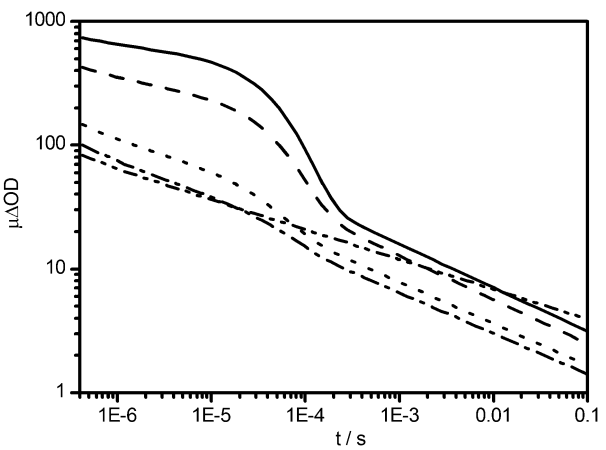

Fig. 7 Fits to eqn (1) of the mass-weighted TAS decays for 10 : 90 (solid line), 20 : 80 (dashed line), 50 : 50 (dotted line), 80 : 20 (dash dotted line), and 100 : 0 (dash dot dotted line) **1** : PS w : w films.

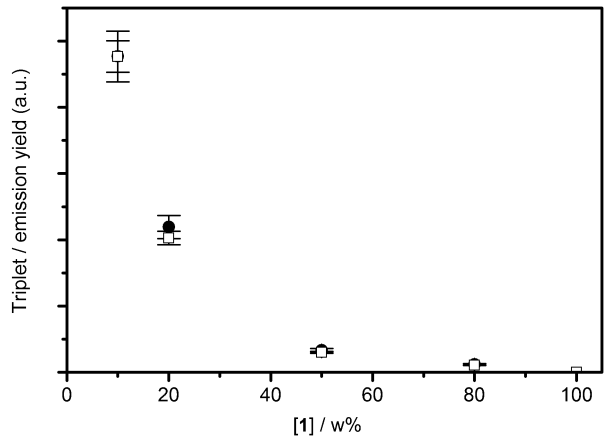

Fig. 8 Normalised plots as a function of weight% **1** in **1** : PS blend films of the C_{60} triplet yield determined from the TAS decays shown in Fig. 7 (solid circles) and of the integrated emission (open squares) determined from the PL data shown in Fig. 5.

Finally we refer to control data investigating the impact of using covalently attached DBA structures *versus* random blend films of the separate donor and acceptor molecules. TAS decays of a neat **1** film and a blend of **2** and **3** were recorded (see Fig. S3 in the ESI†). The neat **1** film showed a yield of charges that is 10 times greater in the blend film. There were no triplets observed in either case.

4. Discussion

The results presented in the previous section give strength to a model with decay pathways from the excited singlet state of C_{60} in **1** as shown in Fig. 9. In this figure the energies of the

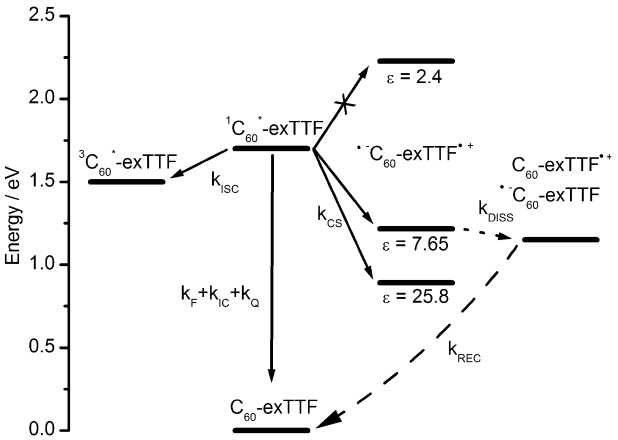

Fig. 9 The energy diagram and kinetic scheme for the DBA molecule (**1**) after generating the C_{60} excited singlet state. From this state the fullerene triplet is formed with a rate constant k_{ISC}, the singlet may also decay to the ground state, either by internal conversion, k_{IC}, or fluorescence, k_F. In the DBA construct the additional pathway of charge separation is added with a rate constant k_{CS}. In the solid state these formed charges may dissociate with a rate constant k_{DISS} and recombine with a rate constant k_{REC}. In addition an alternate decay pathway from the singlet state to the ground state is added through concentration self-quenching, k_Q.

charge separated states were estimated using the Weller equation:[28,29]

$$E_{CS} = E_{1/2}\left(\frac{D^{\bullet+}}{D}\right) - E_{1/2}\left(\frac{A}{A^{\bullet-}}\right) + \frac{e^2}{4\pi\,\varepsilon_0}\left[\left(\frac{1}{2R_+}+\frac{1}{2R_-}-\frac{1}{R_{DA}}\right)\frac{1}{\varepsilon_s} - \left(\frac{1}{2R_+}+\frac{1}{2R_-}\right)\frac{1}{\varepsilon_R}\right] \quad (2)$$

where $E_{\frac{1}{2}}$ is the donor/acceptor oxidation/reduction potential, determined by cyclic voltammetry, ε_S is the relative dielectric constant of the solvent and ε_R the relative dielectric constant of the solvent in which the electrochemical measurements were performed, R_+ and R_- are the average radii of the donor and acceptor, and R_{DA} is the donor–acceptor centre-to-centre distance. R_+ and R_- were estimated from the solvent excluding cavity volume resulting from polarizable continuum model (PCM) calculations, as implemented in Gaussian 03, on geometry optimized structures of unsubstituted exTTF and C_{60} moieties using toluene as solvent. Assuming a spherical cavity this resulted in: $R_+ = 3.25$ Å, and $R_- = 3.65$ Å. R_{DA} was estimated from a structure where the fully geometry optimized exTTF–bridge and C_{60} moieties were connected which resulted in a donor–acceptor center-to-center separation of 22 Å. Cyclic voltammetry data were taken from ref. 35. Fig. 9 shows that, on the basis of these energetic considerations, no charge separation is expected in toluene or in very dilute films of **1** in PS ($\varepsilon \approx 2.4$), consistent with our experimental observations above. As the weight fraction of **1** in PS is increased the average dielectric constant of the film will increase since the value of the pure compound is higher ($\varepsilon \approx 7.65$). Thus, from only considering the effect of dielectric stabilisation, an increasing fraction of charge separation is expected as the concentration of **1** in the films increases.

The validity of eqn (2) in solid thin films might be questionable and more rigorous approaches are planned for future studies. On the other hand, in this case, it seems that eqn (2) is sufficient to approximate the energetics. This was tested by measurements on a very dilute film (2.5 : 97.5) of **1** : PS, which average dielectric constant of 2.5 results in the charge separated state being higher in energy than that of the C_{60} singlet state. For this film only triplets were observed (see Fig. S3 in ESI†). Additionally, measurements were also performed in a more polar polymer, namely PVC ($\varepsilon \approx 3.7$). In this case, all concentrations showed a considerable fraction of long-lived charges (data not shown), consistent with all concentrations resulting in the energy of the charge separated state being lower than that of the C_{60} singlet state.

We employed the kinetic model shown in Fig. 9 to simulate the absorption transients for **1** : PS blend films shown in Fig. 7 (see the ESI† for a description of the fitting procedure). The resulting quantum yields from this fitting procedure are compiled in Fig. 10 together with the normalised signals from triplets and charges (eqn (1)) measured directly at each concentration.

Fig. 10 indicates that as the concentration of **1** in the **1** : PS film is varied, various opposing phenomena are affected. Firstly, as the concentration increases the dielectric constant is increased from almost that of pure PS to that of pure **1**. Thus

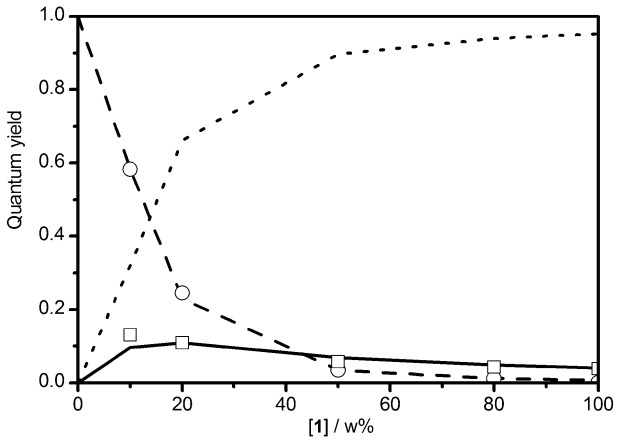

Fig. 10 The calculated quantum yields of charge separation (solid line), C_{60} triplets (dashed line), and the concentration self-quenching process (dotted line). Also shown are the TAS signals corresponding to C_{60} triplets (circles) and exTTF cation radicals (squares) both normalised to fit the respective quantum yield.

the driving force for charge separation increases with increasing concentration which will have a beneficial effect on the charge separation process since the system is in the Marcus normal region. Opposing the beneficial effect of an increasing dielectric constant is the concentration dependent self-quenching of the C_{60} excited state. In line with these opposing forces Fig. 10 shows that the yield of charges initially increases with increasing concentration due to the increased driving force but then decreases with increasing concentration as the self-quenching process gets even more efficient. Thus it seems that the effect of increasing the driving force and providing more pathways for dissociation more or less counteracts the effect of concentration self-quenching. If the latter could be suppressed, an increase in the charge separation yield would instead be observed.

The effect of concentration self-quenching is a well known phenomenon in photophysics of aggregates and solids. Special interest has been focussed on the study of models of the photosynthetic systems.[42–44] Here it has been observed that in closely packed structures, the excited states may span many molecules[34,43] closely resembling Frenkel excitons.[45–48] Self-quenching occurs in a system when domains in the matrix act as traps for the excitation energy.[42,49,50] One may think of this as a simple model for dimerization or excimer formation of two molecules which changes their electronic structure in such a way as to cause fast non-radiative decay channels to develop. The efficiency of quenching is thus dependent on the propensity of forming traps and also the exciton diffusion rate to these traps. The impact of concentration self-quenching on the observed fluorescence life-time and quantum yield is often different.[44,50] This can lead to a large impact on the observed quantum yield with no apparent effect on the fluorescence life-time.[44,50] Many models are concerned with modelling this phenomenon both based on Frenkel excitons and localized excitons. In the context of localized excitons the Förster model has been applied. This relies on the transfer integral which is related to the overlap between the absorption and emission bands. The overlap between the emission and absorption of C_{60} is very small and thus on this grounds a Förster contribution to the exciton diffusion is expected to be low. On the other hand it has been shown that optically forbidden transitions might considerably contribute to the transfer rate and efficiency in large aggregates where molecular separations are not large relative to the molecular dimensions.[48] In summation straightforward approaches to suppress concentration self-quenching are elusive but progress in this area is being made.[51]

In the present case the film morphology might well be made up of well ordered but differing regions, where some might act as a funnel to the ground state. For the DBA molecule studied herein, two very different morphologies have indeed been observed; a 'ball and socket' morphology where the exTTF, which is saddle shaped, holds a C_{60} ball[52–54] and a distinct phase separated morphology where regions of pure exTTF and C_{60}, respectively, are formed.[55] Clearly, in PV devices, the latter of the morphologies is to be preferred, since the donors and acceptors form two phases for transport of holes and electrons, respectively, to the electrodes. A possible means to minimise the occurrence of unwanted intermolecular D/A interactions would be to decorate the different moieties with polar/non-polar groups which would facilitate self-organisation into such a morphology.

Another important property of DBA compounds that has to be taken into account if they are to be used as sole components in photoactive thin films is the intrinsic dielectric constant of the DBA compound itself. To visualize this in terms of formation of the charge separated state and subsequent dissociation into free charge carriers the energy of intermolecular $exTTF^{\bullet+}/C_{60}^{\bullet-}$ as a function of charge separation is plotted in Fig. 11 together with the energy of "free" charges (infinite charge separation minus the thermal energy, 0.026 eV).

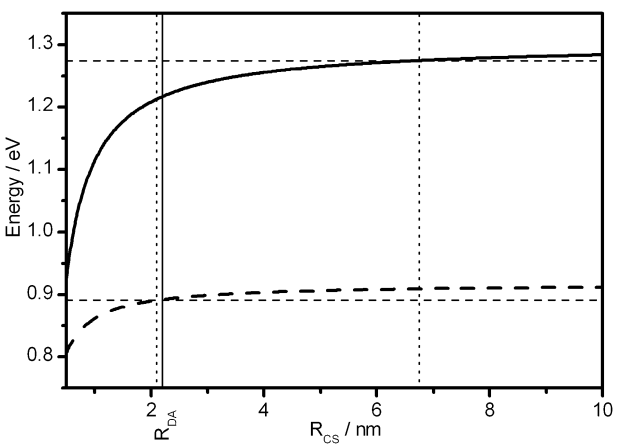

Fig. 11 The calculated energy, using eqn (2), of the intermolecular charge separated state, $exTTF^{\bullet+}/C_{60}^{\bullet-}$, as a function of charge separation in solid film (thick solid curve) and in benzonitrile (thick dashed line). Also shown is the calculated intramolecular donor/acceptor separation, R_{DA} = 22 Å (thin vertical solid line). Also indicated is the distances (vertical dashed lines) and energies (horizontal dashed lines) where the calculated energy of the charge separated state is less than k_BT (the thermal energy), lower than the energy at infinite separation. At this energy the electron and hole can be considered to be free.

From this figure it can be seen that for a dielectric constant similar to that of a benzonitrile solution the charges generated in the intramolecular ET step have broken the coulomb binding immediately when they are formed. On the other hand, for a dielectric constant similar to that of a solid film of **1** the formed intramolecular charges are moderately bound ($\sim$0.2 eV), indicating that intermolecular rather than intramolecular charge separation is necessary to overcome the coulomb attraction of the charge pair. This barrier is estimated for a fully relaxed DBA system with its surrounding medium. Thus the barrier might be smaller in case of slower structural reorganization and thermalization in the solid state.[56] This suggests that a fine tuning of the electronic coupling and donor–acceptor separation together with knowledge of the dielectric properties of the DBA compound itself is the way to optimize the yield of free charges in films incorporating DBA compounds. Additionally, to improve the efficiencies of solar cells based on this type of construct, self-organising schemes are needed to favour intermolecular D/D and A/A interactions, whilst at the same time minimising intermolecular D/A interactions which may result in enhanced recombination losses. One such motif might be to decorate one of the moieties with more polar groups and the other with less polar groups. When an appropriate morphology has been achieved it is important to choose a bridge length so that the charges might break the coulomb barrier in the charge separation step. In this respect it is possible that DBA compounds incorporating either an ionic donor or acceptor might be beneficial, since this will lead to a charge separation step that is more of a charge shift character and will thus lead to a less bound charge separated state.

5. Conclusions

A fullerene based DBA compound, incorporating a π-extended tetrathiafulvalene electron donor, was investigated with respect to its photophysics in solution *versus* solid state thin films. In a previous study it was concluded that the intramolecular electronic coupling between a donor and an acceptor was much too large in relation to the intermolecular electronic coupling between donor/donor and acceptor/acceptor.[1] In the present study the DBA compound had a more moderate intramolecular electronic coupling and also a larger donor–acceptor separation. This was found to increase the charge generation yield in the film of the DBA compound, **1**, in comparison to a film of a mixture of the donor and acceptor reference compounds, **2** and **3**. Further, it was shown that the fullerene is subjected to concentration self-quenching, which was found to severely reduce the charge transfer yield in solid state relative to solution. This suggests that concentration self-quenching is a reason why solar cells made from dyads relying on charge transfer from photo-excited fullerenes have not reached high efficiencies. In line with this, attempts to make devices based on pristine films of **1** did not achieve any appreciable efficiency. The present study also highlighted that in the solid state, it is important to take account of dielectric stabilisation. Thus an additional molecular property that can aid in the design of DBA systems that function efficiently in the solid state is introduced.

Acknowledgements

Further support from the UK EPSRC's Supergen and Nanotechnology Grand Challenge programmes is gratefully acknowledged. M. P. E. is thankful to the Knut and Alice Wallenberg Foundation for funding. Financial support by the MICINN of Spain (CTQ2008-00795/BQU), the ESF (SOHYD MAT2006-28170-E), the FUNMOLS (FP7-212942-2), the CAM (MADRISOLAR-2 S2009/PPQ-1533), and the European FEDER funds is acknowledged. A. M. O. and A. G. thank the CAM, and the MEC of Spain for a research grant and a Ramón y Cajal contract, respectively.

Notes and references

1 S. Shoaee, M. P. Eng, Z. S. An, X. Zhang, S. Barlow, S. R. Marder and J. R. Durrant, *Chem. Commun.*, 2008, 4915–4917.
2 S. Handa, F. Giacalone, S. A. Haque, E. Palomares, N. Martin and J. R. Durrant, *Chem.–Eur. J.*, 2005, **11**, 7440–7447.
3 N. Camaioni, G. Fabbrini, E. Menna, M. Maggini, G. Ridolfi and A. Zanelli, *New J. Chem.*, 2006, **30**, 335–342.
4 J. F. Eckert, J. F. Nicoud, J. F. Nierengarten, S. G. Liu, L. Echegoyen, F. Barigelletti, N. Armaroli, L. Ouali, V. Krasnikov and G. Hadziioannou, *J. Am. Chem. Soc.*, 2000, **122**, 7467–7479.
5 A. Gouloumis, A. de la Escosura, P. Vazquez, T. Torres, A. Kahnt, D. M. Guldi, H. Neugebauer, C. Winder, M. Drees and N. S. Sariciftci, *Org. Lett.*, 2006, **8**, 5187–5190.
6 D. M. Guldi, C. P. Luo, A. Swartz, R. Gomez, J. L. Segura, N. Martin, C. Brabec and N. S. Sariciftci, *J. Org. Chem.*, 2002, **67**, 1141–1152.
7 J. L. Hua, F. S. Meng, F. Ding, F. Y. Li and H. Tian, *J. Mater. Chem.*, 2004, **14**, 1849–1853.
8 M. A. Loi, P. Denk, H. Hoppe, H. Neugebauer, C. Winder, D. Meissner, C. Brabec, N. S. Sariciftci, A. Gouloumis, P. Vazquez and T. Torres, *J. Mater. Chem.*, 2003, **13**, 700–704.
9 M. Maggini, G. Possamai, E. Menna, G. Scorrano, N. Camaioni, G. Ridolfi, G. Casalbore-Miceli, L. Franco, M. Ruzzi and C. Corvaja, *Chem. Commun.*, 2002, 2028–2029.
10 F. S. Meng, J. L. Hua, K. C. Chen, H. Tian, L. Zuppiroli and F. Nuesch, *J. Mater. Chem.*, 2005, **15**, 979–986.
11 M. Narutaki, K. Takimiya, T. Otsubo, Y. Harima, H. M. Zhang, Y. Araki and S. Ito, *J. Org. Chem.*, 2006, **71**, 1761–1768.
12 J. F. Nierengarten, J. F. Eckert, J. F. Nicoud, L. Ouali, V. Krasnikov and G. Hadziioannou, *Chem. Commun.*, 1999, 617–618.
13 E. Peeters, P. A. van Hal, J. Knol, C. J. Brabec, N. S. Sariciftci, J. C. Hummelen and R. A. J. Janssen, *J. Phys. Chem. B*, 2000, **104**, 10174–10190.
14 A. Possamai, N. Camaioni, G. Ridolfi, L. Franco, M. Ruzzi, E. Menna, G. Casalbore-Miceli, A. M. Fichera, G. Scorrano, C. Corvaja and M. Maggini, *Synth. Met.*, 2003, **139**, 585–588.
15 G. Possamai, M. Maggini, E. Menna, G. Scorrano, L. Franco, M. Ruzzi, C. Corvaja, G. Ridolfi, P. Samori, A. Geri and N. Camaioni, *Appl. Phys. A: Mater. Sci. Process.*, 2004, **79**, 51–58.
16 G. Possamai, S. Marcuz, M. Maggini, E. Menna, L. Franco, M. Ruzzi, S. Ceola, C. Corvaja, G. Ridolfi, A. Geri, N. Camaioni, D. M. Guldi, R. Sens and T. Gessner, *Chem.–Eur. J.*, 2005, **11**, 5765–5776.
17 M. R. Wasielewski, *J. Org. Chem.*, 2006, **71**, 5051–5066.
18 N. Martin, L. Sanchez, M. A. Herranz, B. Illescas and D. M. Guldi, *Acc. Chem. Res.*, 2007, **40**, 1015–1024.
19 A. Kahnt, D. M. Guldi, A. de la Escosura, M. V. Martin-Diaz and T. Torres, *J. Mater. Chem.*, 2008, **18**, 77–82.
20 S. Amthor and C. Lambert, *J. Phys. Chem. A*, 2006, **110**, 1177–1189.
21 A. de la Escosura, M. V. Martinez-Diaz, P. Thordarson, A. E. Rowan, R. J. M. Nolte and T. Torres, *J. Am. Chem. Soc.*, 2003, **125**, 12300–12308.
22 L. Sanchez, I. Perez, N. Martin and D. M. Guldi, *Chem.–Eur. J.*, 2003, **9**, 2457–2468.
23 D. M. Guldi and M. Prato, *Acc. Chem. Res.*, 2000, **33**, 695–703.
24 S. Cook, H. Ohkita, Y. Kim, J. J. Benson-Smith, D. D. C. Bradley and J. R. Durrant, *Chem. Phys. Lett.*, 2007, **445**, 276–280.

25 N. Minami, S. Kazaoui and R. Ross, *Synth. Met.*, 1995, **70**, 1397–1400.
26 Q. S. Xie, F. Arias and L. Echegoyen, *J. Am. Chem. Soc.*, 1993, **115**, 9818–9819.
27 Y. Kim, S. Cook, S. M. Tuladhar, S. A. Choulis, J. Nelson, J. R. Durrant, D. D. C. Bradley, M. Giles, I. McCulloch, C. S. Ha and M. Ree, *Nat. Mater.*, 2006, **5**, 197–203.
28 A. Weller, *Z. Phys. Chem., Neue Folge*, 1982, **133**, 93–98.
29 A. Weller and D. Rehm, *Ber. Bunsen-Ges. Phys. Chem.*, 1969, **73**, 834–839.
30 T. Jeffrey, *Tetrahedron Lett.*, 1985, **26**, 2667–2670.
31 M. Maggini, G. Scorrano and M. Prato, *J. Am. Chem. Soc.*, 1993, **115**, 9798–9799.
32 N. Tagmatarchis and M. Prato, *Synlett*, 2003, 768–779.
33 M. J. Frisch, G. W. Trucks, H. B. Schlegel, G. E. Scuseria, M. A. Robb, J. R. Cheeseman, J. A. Montgomery, T. K. Vreven, K. N. Kudin, J. C. Burant, J. M. Millam, S. S. Iyengar, J. Tomasi, V. Barone, B. Mennucci, M. S. Cossi, G. N. Rega, G. A. Petersson, H. Nakatsuji, M. Hada, M. Ehara, K. Toyota, R. Fukuda, J. Hasegawa, M. Ishida, T. Nakajima, Y. Honda, O. Kitao, H. Nakai, M. Klene, X. Li, J. E. Knox, H. P. Hratchian, J. B. Cross, C. Adamo, J. Jaramillo, R. Gomperts, R. E. Stratmann, O. Yazyev, A. J. Austin, R. Cammi, C. Pomelli, J. W. Ochterski, P. Y. Ayala, K. Morokuma, G. A. Voth, P. Salvador, J. J. Dannenberg, V. G. Zakrzewski, S. Dapprich, A. D. Daniels, M. C. Strain, O. Farkas, D. K. Malick, A. D. Rabuck, K. Raghavachari, J. B. Foresman, J. V. Ortiz, Q. Cui, A. G. Baboul, S. Clifford, J. Cioslowski, B. B. Stefanov, G. Liu, A. Liashenko, P. Piskorz, I. Komaromi, R. L. Martin, D. J. Fox, T. Keith, M. A. Al-Laham, C. Y. Peng, A. Nanayakkara, M. Challacombe, P. M. W. Gill, B. Johnson, W. Chen, M. W. Wong, C. Gonzalez and J. A. Pople, Gaussian, Inc., Pittsburgh PA, 2003.
34 J. Moll, S. Daehne, J. R. Durrant and D. A. Wiersma, *J. Chem. Phys.*, 1995, **102**, 6362–6370.
35 D. M. Guldi, F. Giacalone, G. de la Torre, J. L. Segura and N. Martin, *Chem.–Eur. J.*, 2005, **11**, 7199–7210.
36 M. C. Diaz, M. A. Herranz, B. M. Illescas, N. Martin, N. Godbert, M. R. Bryce, C. P. Luo, A. Swartz, G. Anderson and D. M. Guldi, *J. Org. Chem.*, 2003, **68**, 7711–7721.
37 W. Seitz, A. Kahnt, D. M. Guldi and T. Torres, *J. Porphyrins Phthalocyanines*, 2009, **13**, 1034–1039.
38 M. Wielopolski, C. Atienza, T. Clark, D. M. Guldi and N. Martin, *Chem.–Eur. J.*, 2008, **14**, 6379–6390.
39 J. Nelson, *Phys. Rev. B: Condens. Matter*, 2003, **67**, 155209.
40 T. A. Ford, H. Ohkita, S. Cook, J. R. Durrant and N. C. Greenham, *Chem. Phys. Lett.*, 2008, **454**, 237–241.
41 H. Ohkita, S. Cook, Y. Astuti, W. Duffy, M. Heeney, S. Tierney, I. McCulloch, D. D. C. Bradley and J. R. Durrant, *Chem. Commun.*, 2006, 3939–3941.
42 G. S. Beddard and G. Porter, *Nature*, 1976, **260**, 366–367.
43 J. R. Durrant, D. R. Klug, S. L. S. Kwa, R. Vangrondelle, G. Porter and J. P. Dekker, *Proc. Natl. Acad. Sci. U. S. A.*, 1995, **92**, 4798–4802.
44 A. R. Kelly and L. K. Patterson, *Proc. R. Soc. London, Ser. A*, 1971, **324**, 117–126.
45 H. Fidder, J. Terpstra and D. A. Wiersma, *J. Chem. Phys.*, 1991, **94**, 6895–6907.
46 R. P. Hemenger and R. M. Pearlstein, *Chem. Phys.*, 1973, **2**, 424–432.
47 R. M. Pearlstein, *J. Chem. Phys.*, 1972, **56**, 2431–2442.
48 G. D. Scholes, X. J. Jordanides and G. R. Fleming, *J. Phys. Chem. B*, 2001, **105**, 1640–1651.
49 J. Knoester and J. E. Vanhimbergen, *J. Chem. Phys.*, 1987, **86**, 3571–3576.
50 A. Penzkofer and Y. Lu, *Chem. Phys.*, 1986, **103**, 399–405.
51 W. Z. Yuan, P. Lu, S. Chen, J. W. Y. Lam, Z. Wang, Y. Liu, H. S. Kwok, Y. Ma and B. Z. Tang, *Adv. Mater.*, 2010, **22**, 2159–2163.
52 G. Fernandez, E. M. Perez, L. Sanchez and N. Martin, *J. Am. Chem. Soc.*, 2008, **130**, 2410–2411.
53 G. Fernandez, E. M. Perez, L. Sanchez and N. Martin, *Angew. Chem., Int. Ed.*, 2008, **47**, 1094–1097.
54 G. Fernandez, L. Sanchez, E. M. Perez and N. Martin, *J. Am. Chem. Soc.*, 2008, **130**, 10674–10683.
55 R. Otero, D. Ecija, G. Fernandez, J. M. Gallego, L. Sanchez, N. Martin and R. Miranda, *Nano Lett.*, 2007, **7**, 2602–2607.
56 T. M. Clarke, A. M. Ballantyne, J. Nelson, D. D. C. Bradley and J. R. Durrant, *Adv. Funct. Mater.*, 2008, **18**, 4029–4035.